Passive scalar fluctuations with and without a mean gradient: A numerical study

Emily S. C. Ching*
Institute for Theoretical Physics, University of California, Santa Barbara, Santa Barbara, California 93106

Yuhai Tu
California Institute of Technology, Pasadena, California 91125
(Received 16 August 1993)

We report a numerical study of a passive scalar advected by a random incompressible Gaussian velocity field. The calculations are carried out on a two-dimensional square lattice. Depending on the two dimensionless parameters in the problem, the scalar fluctuations at the center can be Gaussian, exponential, or stretched exponential. This is true not only when the passive scalar is subjected to a uniform mean gradient but also true when a new alternating boundary condition is used which results in a mean scalar profile that has a vanishing gradient in the central region.

PACS number(s): 47.27.−i, 02.50.−r, 05.40.+j

I. INTRODUCTION

Recent experiments [1] on Rayleigh-Bénard convection in low-temperature helium gas revealed that the probability density function (PDF) of temperature fluctuations measured at the center of the cell is non-Gaussian and close to exponential (sometimes high-pas filtering [2] is required to get the exponential) when Rayleigh number is large ($\leq 10^8$). This discovery of nearly exponential temperature fluctuations in convection has stimulated many recent studies on PDF's [3–10].

In their work, Pumir, Shraiman, and Siggia (PSS) [5] suggested that buoyancy effects are not necessary for the exponential tails in these experiments. Using a one-dimensional phenomenological model equation for passive scalar PDF's, they obtained steady-state solutions with exponential tails in the case where the scalar has a uniform mean gradient. Although their model is not systematically derived, it is argued to contain the physics of random advection and mixing. Thus they predicted that random advection and mixing plus the existence of a uniform mean gradient provide a mechanism for production of exponentials. Their prediction has recently found both numerical [11] and experimental support [12,13]. However, its relevance to the observations mentioned above [1] is not clear since the central region in the convection experiment is well mixed with the temperature change concentrated in two thermal boundary layers near the top and the bottom of the cell [14]. One is thus led to the following natural question: Can passive scalar fluctuations still possess exponential tails in the absence of a local mean gradient?

In this paper, we report results from a numerical study that addresses this question. We shall see that the answer is positive and that random advection and diffusion can produce exponential tails even in the absence of a local mean gradient. As a result, we believe that the same physics produce the exponential PDF's observed in the convection experiments [1].

II. PROBLEM

We study the random advection and diffusion of a passive scalar. The governing equations are

$$\frac{\partial T}{\partial t}+\mathbf{u}\cdot\nabla T=D_0\nabla^2 T\ , \tag{1a}$$

$$\nabla\cdot\mathbf{u}=0\ , \tag{1b}$$

where $T(\mathbf{x},t)$ is a passive scalar, e.g., the temperature field and $\mathbf{u}(\mathbf{x},t)$ is the velocity field with D_0 being the molecular diffusivity. We restrict ourselves to two dimensions where the incompressible velocity field is expressed using the stream function $\phi(\mathbf{x},t)$: $u_x=\partial_y\phi$, $u_y=-\partial_x\phi$. To mimic a turbulent velocity field, we model the stream function $\phi(\mathbf{x},t)$ (and thus the velocity field) as a Gaussian random field with correlation length ξ, correlation time τ, and the noise strength ϕ_0.

Instead of solving the full advection-diffusion problem in Eq. (1), we resort to a simplified discrete model which is coarse grained at the scale of the velocity correlation length ξ. That is, we solve Eq. (1) on a two-dimensional square lattice with a lattice spacing equals to ξ. The coarse-graining effectively renormalizes the molecular transport coefficient so we replace D_0 by an effective eddy diffusivity D. Using the following transformations: $t\rightarrow\tau t$, $\mathbf{x}\rightarrow\xi\mathbf{x}$, $\mathbf{u}\rightarrow u_0\mathbf{u}$ ($u_0=\phi_0/\xi$), we rewrite Eq. (1a) (with D_0 replaced by D) in a dimensionless form

$$\frac{\partial T(i,j)}{\partial t}+K\mathbf{u}(i,j)\cdot\nabla_{ij}T=C^{-1}\nabla_{ij}^2T(i,j)\ , \tag{2}$$

with two parameters K and C, where K is the Kubo number [15] identically equal to $u_0\tau/\xi$ and $C=\xi^2/(D\tau)$. We use the finite-difference method to integrate Eq. (2) in time. A small time step Δt is used with the random ve-

*Present address: Department of Physics, The Chinese University of Hong Kong, Hong Kong.

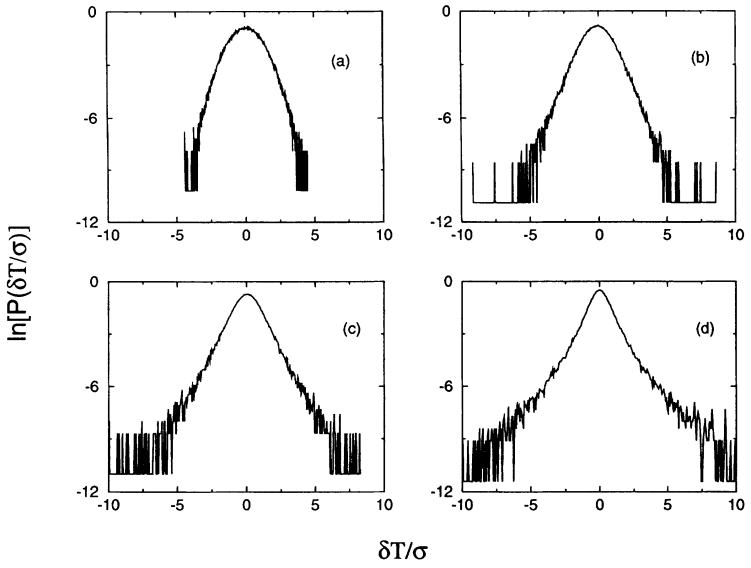

FIG. 1. PDF's for different values of C at $K=1$ for the fixed-difference boundary condition. (a) $C=2$, Gaussian PDF; (b) $C=\frac{20}{3}$, PDF with exponential tail; (c) $C=9$, nearly pure exponential PDF; (d) $C=\frac{40}{3}$, stretched-exponential PDF (the stretched exponent $\beta\sim 0.65$, see text for definition).

locity field $\mathbf{u}$ (or the random stream function ϕ) at each lattice site being updated every N $(=\tau/\Delta t)$ time steps. The system size is $N_1\times N_2$ and $N_1=N_2=31$ is used in this work. The boundary condition for both the velocity and the temperature is periodic in the horizontal direction (i direction), and the velocity field is no-slip on both the top and bottom boundaries ($j=0$ and N_2+1). Several different boundary conditions on temperature in the j direction are employed. The first one is the usual "fixed-difference" condition with $T(i,j=0)=0$ and $T(i,j=N_2+1)=1$. With this boundary condition, the scalar has a uniform mean gradient in the j direction. In order to obtain a mean scalar profile that has a vanishing gradient at the center of the system, we use a new "alternating boundary condition." Finally, to relate to the convection experiment, we use a third "random boundary condition." These boundary conditions will be described in detail below. For each of these boundary conditions, we measure temperature as a function of time and study the statistics of fluctuations at the center of the system $[\frac{1}{2}(N_1+1),\frac{1}{2}(N_2+1)]$. Each time series consists of at least 150 000 points.

III. RESULTS

A. Fixed-difference boundary condition

We first consider the situation in which a fixed temperature difference is applied across the system, i.e.,

$$T(i,j=0,t)=0,\quad T(i,j=N_2+1,t)=1\ ,\qquad i=1,\ldots,N_1\ . \tag{3}$$

For all the values of K and C studied, the mean temperature profile is found to be linear in the j direction with a gradient of $1/(N_2+1)$. At a fixed value of K, the PDF is Gaussian for small values of C and becomes non-Gaussian by developing exponential tails as C is increased. When C is increased further, the exponential part of the PDF extends towards the center of the distribution, and at $C=C_*$, the whole PDF becomes almost exponential. For $C>C_*$, the PDF eventually becomes stretched exponential, i.e., $P(\delta T)\sim\exp[-A(\delta T)^\beta]$ with $\beta<1$, where $\delta T=T-\langle T\rangle$ is the fluctuation around the time-averaged mean. In Fig. 1 we show PDF's at different stages for $K=1$ (which is essentially the case considered by PSS, where τ was taken to be $\sim\xi/u_0$). The fluctuations are normalized by the standard deviation σ. We repeat the calculations for different values of K's and construct the phase diagram shown in Fig. 2. We divide the whole parameter space into three regions which correspond, respectively, to Gaussian (G) PDF's, PDF's with exponential tail (ET), and stretched-exponential (SE) PDF's. In determining the boundaries between different regions, we have used the kurtosis $F=\langle(\delta T)^4\rangle/\langle(\delta T)^2\rangle^2$, and the three regions are classified by the following criteria: $F=3$–3.2 for the G region, $3.2<F<6$ for the ET region, and $F>6$ for the SE region. In Fig. 3, we plot the kurtosis F as a function of C for $K=1$.

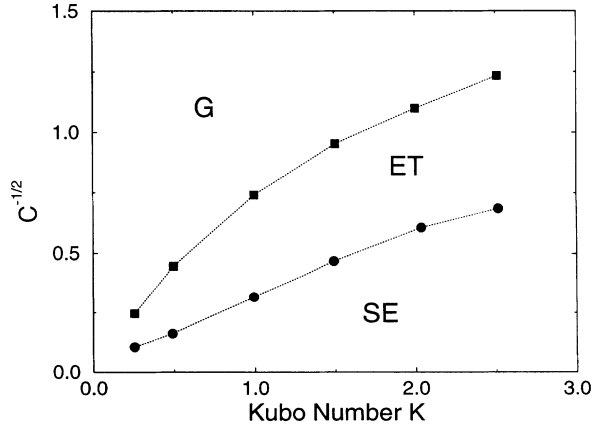

FIG. 2. Phase diagram in the $\{K,C\}$ plane for the fixed-difference boundary condition.

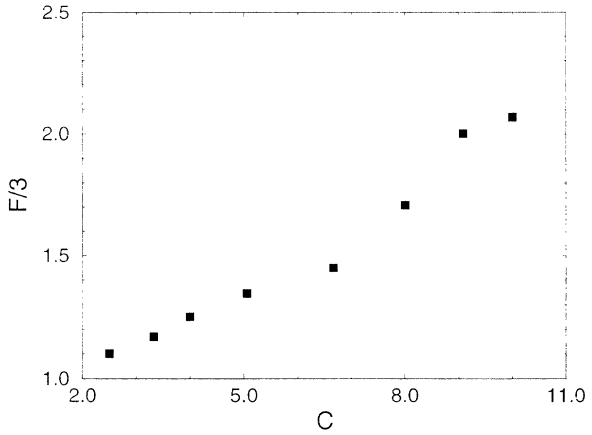

FIG. 3. $F/3$ versus C for $K=1$ for the fixed-difference boundary condition.

B. Alternating boundary condition

To create the situation where the scalar has a vanishing mean gradient at the center, we introduce a new alternating temperature boundary condition

$$T(i,j=0,t)=T(i,j=N_2+1,t)=10(-1)^{i+1}\ ,$$
$$i=1,\ldots,N_1\ . \quad (4)$$

As shown in Fig. 4, the resulted mean temperature profile is quite different from before. It is almost flat for most of the system except for regions near the top and the bottom boundaries. We find that the mean profile only changes slightly upon variation of K and C. As before, we study the statistics of temperature fluctuations at the center. Although the mean gradient vanishes at the center, we find a phase diagram qualitatively similar to the previous case: at a fixed value of K, the PDF becomes non-Gaussian for large enough values of C. In Fig. 5, we plot F as a function of C for $K=1$. Comparing to Fig. 3, the deviation of F from 3 occurs more abruptly and at a larger value of C. For this alternative boundary condition, when the PDF's become non-Gaussian, they are also more skewed, thus F, by itself, may not be a good quantitative measure of how non-Gaussian the PDF is. Figure 5 clearly demonstrates that a uniform mean gradient is not necessary for generating non-Gaussian passive scalar fluctuations. Moreover, since the mean temperature gradient vanishes at the center, we have shown that exponential tails can still exist in the absence of a local mean gradient. In Fig. 6, we compare three PDF's for $K=1$ and $C=10$: two measured at the center, one for each of the two boundary conditions, fixed-difference and alternating [Eqs. (3) and (4)], and the third one off the midplane, measured at $[\frac{1}{2}(N_1+1),\frac{1}{4}(N_2+1)]$ for the alternating boundary condition Eq. (4). These results therefore suggest that whether the statistics of the fluctuations is Gaussian or not does not depend on the shape of the mean scalar profile but is mainly determined by the parameters K and C.

C. Random boundary condition

To relate to the convection experiments, we look at another boundary condition

$$T(i,j=0,t)=T(i,j=N_2+1,t)=\eta(i)\ ,$$
$$i=1,\ldots,N_1 \quad (5)$$

with η being a Gaussian random number of zero mean and unit variance. This random boundary condition is motivated by the fluctuating thermal boundaries observed in experiments. Here the boundaries we have in mind are not the top and bottom plates of the experimental cell but rather the top and bottom of the central well-mixed region inside the cell. With this random boundary condition, qualitatively similar results are again found as can be seen from the plot of F versus C shown also in Fig. 5. Note that the values of F will change for different realizations of η. In the actual experiment, the thermal boundaries also fluctuate in time. It is therefore interesting to study the effects of time variation in Eq. (5). However, if we simply update the boundaries randomly, we

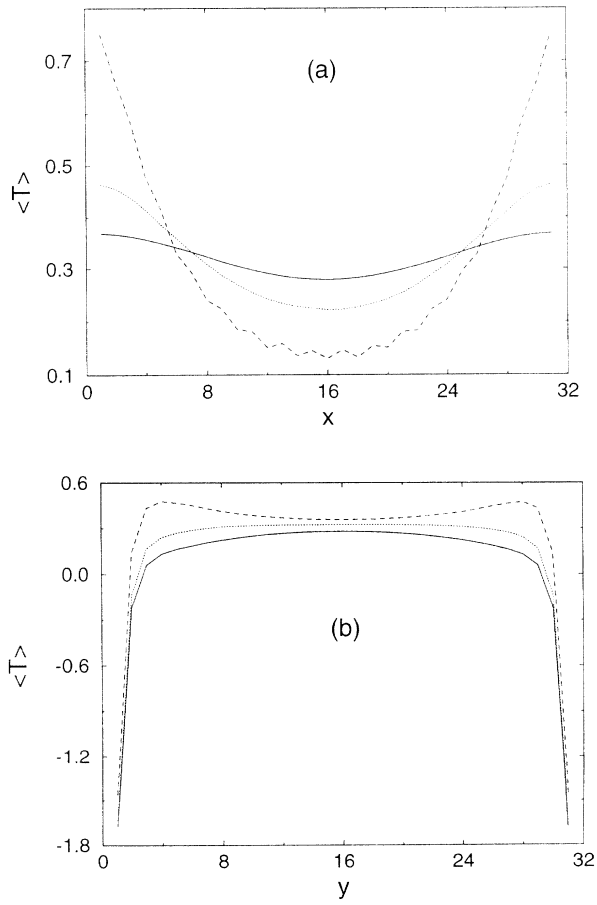

FIG. 4. Mean temperature profile for the alternating boundary condition Eq. (4) with $K=1$ and $C=10$ (a) along the x direction at $y=4$ (dashed line), $y=8$ (dotted line), and $y=16$ (solid line); (b) along the y direction at $x=4$ (dashed line), $x=8$ (dotted line), and $x=16$ (solid line). It is symmetric with respect to the lines $x=16$ and $y=16$.

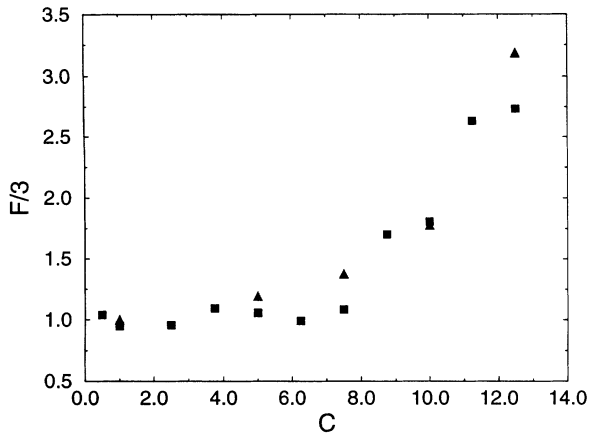

FIG. 5. $F/3$ versus C with $K=1$ for the alternating boundary condition Eq. (4) (squares) and the random boundary condition Eq. (5) (triangles).

will inevitably get Gaussian PDF's as a result of averaging over a large number of independent random conditions. With no better clues to the actual dynamics of the thermal boundaries, we study the time variation in the following simple way: updating the boundaries every M ($=10, 100, 1000, 10\,000$) time steps by adding a small random number (of noise strength 0.001) to the previous values. We find that the exponential tails still persist for $M \geq 1000$, but the PDF becomes more Gaussian as M decreases.

IV. DISCUSSION AND CONCLUSIONS

We have studied numerically the problem of a passive scalar advected by a random velocity field. Depending on the two dimensionless parameters K and C in the problem, the PDF of passive scalar fluctuations can be Gaussian, non-Gaussian developing exponential tails, exponential, and even stretched exponential. This is true for all the three different boundary conditions considered even for the case in which the mean scalar profile has a vanishing gradient at the center.

To put our results into perspective, we relate the parameters K and C to the Péclet number (Pe). With Pe defined as $u\xi/D_0$, we have $\mathrm{Pe}=KC(D/D_0)$. On purely dimensional grounds, one expects $D \approx D_0 \mathrm{Pe}^{\nu}$ when $\mathrm{Pe} \gg 1$, with the exponent ν depending on the topology of the flow. Thus we get $\mathrm{Pe}=(KC)^{1/(1-\nu)}$. For two-dimensional, steady, incompressible, random flows, ν was derived [16] to be $\frac{10}{13}$. This particular value may not apply in our case as our velocity field is not steady. Indeed, determining ν for different physical situations is nontrivial and is a problem of its own interest [17]. Nevertheless, it is well possible that even in our case, ν is close to but less than 1 and large KC implies large Pe. In real experiments, a certain path in the $\{K,C\}$ space is traced depending on how Pe is varied.

Our results for the fixed-difference boundary condition confirm PSS's prediction [5] that in the presence of a uniform mean temperature gradient α ($\langle T \rangle = a + \alpha y$) and with large enough Péclet number, the PDF should have an exponential tail: $P(\delta T) \sim \exp(-|\delta T|/\gamma)$ for $|\delta T| \gg 1$. According to PSS, the length scale L, defined by γ/α, should be equal to the velocity correlation length ξ. However, in Fig. 7 we plot L/ξ vs C for $K=1$ and find that L/ξ actually depends on C. It is less than 1 for $C < C_*$ and approaches 1 as $C \to C_*$. In addition, the appearance of the stretched-exponential region beyond C_* is unpredicted by the phenomenological model of PSS. These results suggest that the PSS model corresponds only to the case when C is approximately C_*. We should mention that stretched-exponential temperature PDF's have not been reported in experiments, but if ν is very close to 1, then they can only be observed at very large Péclet number.

Initiated by the work of PSS, two experiments [12,13] have been performed to study passive temperature fluctuations. In a wind tunnel experiment, Jayesh and Warhaft [12] found exponential PDF's when a mean tem-

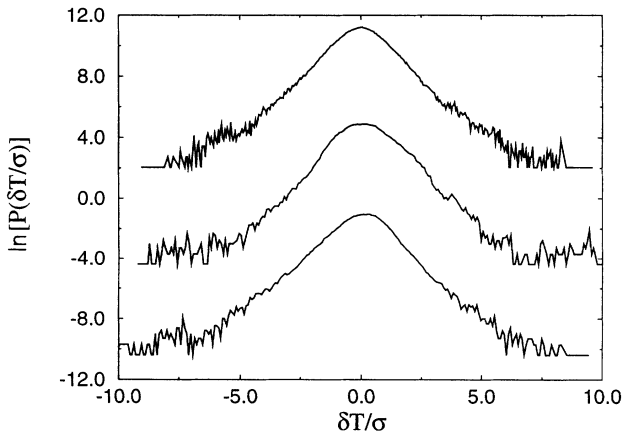

FIG. 6. Temperature PDF's for $K=1$ and $C=10$. The upper two PDF's have been shifted upwards by 12 and 6, respectively, and are measured at the center $[\frac{1}{2}(N_1+1), \frac{1}{2}(N_2+1)]$, with the uppermost one using boundary condition Eq. (3) and the lower one using Eq. (4). The lowest PDF is measured at $[\frac{1}{2}(N_1+1), \frac{1}{4}(N_2+1)]$ using boundary condition Eq. (4).

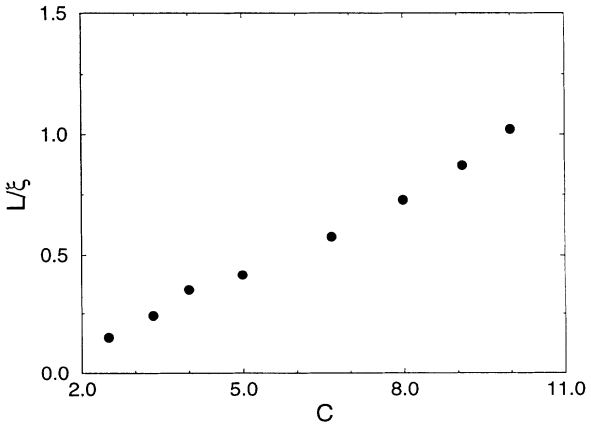

FIG. 7. L/ξ versus C for $K=1$ for the fixed-difference boundary condition.

perature gradient was maintained by differentially heating a set of parallel heating ribbons (a toaster) placed at the entrance. To study the situation in the absence of a mean gradient, they used an array of fine heated wires (a mandoline) and observed PDF's which are closer to Gaussian (though skewed with "enhanced" tails on the positive side). Since all the wires are equally heated, we think that the mandoline may not be a good source of temperature fluctuations. A better way may be to heat the set of toaster ribbons alternately as in Eq. (4). It will be interesting to see how the corresponding PDF's look like and whether they agree with what we have found. In another experiment, Gollub *et al.* [13] studied temperature fluctuations in a fluid stirred by an oscillating grid. A fixed horizontal temperature difference was maintained across the experimental cell. Thus their experimental setup is close to the situation we have studied here [with boundary condition Eq. (3)]. In particular, K is fixed when the Reynolds number (Re) is increased so C is proportional to $\mathrm{Re}^{1-\nu}$. They found that the PDF is Gaussian when Re is small and becomes exponential when Re is larger. We note here the close resemblance of their plot of kurtosis as a function of Reynolds number (Fig. 6 in their paper) to our Fig. 3. Again, it will be interesting to study how the PDF changes when a different boundary condition such as Eq. (4) is introduced.

In summary, we find that as long as there is a source of scalar fluctuations, provided by the boundaries in some ways, the PDF of a passive scalar undergoing random advection will have exponential tails whenever the Péclet number is large enough. This is true no matter what the shape of the local mean scalar profile is. It was mentioned in several papers [12,13] that exponential tails in the absence of a mean gradient were observed before in a spectral large-eddy simulation [18]. We would like to point out that those PDF's observed are transients while ours are steady-state results and are therefore more relevant to experimental observations. We therefore suggest that the exponential PDF's observed in convection [1] are caused by the same physics: random advection and mixing, which produce the exponential passive scalar PDF's observed here and in the passive scalar experiments [12,13].

ACKNOWLEDGMENTS

We thank J. Carlson, L. P. Kadanoff, J. Langer, and F. Liu for discussions. The work at Santa Barbara is supported in part by the National Science Foundation Grant No. PHY89-04035. Y.T. would like to acknowledge support by the California Institute of Technology.

[1] F. Heslot, B. Castaing, and A. Libchaber, Phys. Rev. A **36**, 5870 (1987); B. Castaing *et al.*, J. Fluid Mech. **204**, 1 (1989); M. Sano, X.-Z. Wu, and A. Libchaber, Phys. Rev. A **40**, 6421 (1989).
[2] X.-Z. Wu and A. Libchaber, Phys. Rev. A **45**, 842 (1992).
[3] Y. G. Sinai and V. Yakhot, Phys. Rev. Lett. **63**, 1962 (1989).
[4] V. Yakhot, Phys. Rev. Lett. **63**, 1965 (1989).
[5] A. Pumir, B. I. Shraiman, and E. D. Siggia, Phys. Rev. Lett. **66**, 2984 (1991).
[6] H. Chen, S. Chen, and R. H. Kraichnan, Phys. Rev. Lett. **63**, 2657 (1989); R. H. Kraichnan, *ibid.* **65**, 575 (1990).
[7] Z.-S. She, Phys. Rev. Lett. **66**, 600 (1991); Z.-S. She and S. A. Orszag, *ibid.* **66**, 1701 (1991).
[8] E. S. C. Ching, Phys. Rev. Lett. **70**, 283 (1993).
[9] S. B. Pope and E. S. C. Ching, Phys. Fluids A **5**, 1529 (1993).
[10] Y. Kimura and R. H. Kraichnan, Phys. Fluids A **5**, 2276 (1993).
[11] M. Holzer and A. Pumir, Phys. Rev. E **47**, 202 (1993).
[12] Jayesh and Z. Warhaft, Phys. Rev. Lett. **67**, 3503 (1991); Phys. Fluids A **4**, 2292 (1992).
[13] J. P. Gollub *et al.*, Phys. Rev. Lett. **67**, 3507 (1991); B. R. Lane *et al.*, Phys. Fluids A **5**, 2255 (1993).
[14] A. Belmonte, A. Tilgner, and A. Libchaber, Phys. Rev. Lett. **70**, 4067 (1993).
[15] R. Kubo, J. Math. Phys. **4**, 174 (1963).
[16] A. V. Gruzinov, M. B. Isichenko, and Y. L. Kalda, Zh. Eksp. Teor. Fiz. **97**, 476 (1989) [Sov. Phys. JETP **69**, 517 (1989)].
[17] M. B. Isichenko, Rev. Mod. Phys. **64**, 961 (1992).
[18] O. Metais and M. Lesieur, J. Fluid Mech. **239**, 157 (1992).